

Solubility of three natural compounds with insecticidal activity in supercritical carbon dioxide:
Experimental measurements and predictive modeling with the GC-EoS

Original

Solubility of three natural compounds with insecticidal activity in supercritical carbon dioxide: Experimental measurements and predictive modeling with the GC-EoS / Mazzei, H.; Ortega, L.; Andreatta, A. E.; Ganan, N. A.. - In: FLUID PHASE EQUILIBRIA. - ISSN 0378-3812. - ELETTRONICO. - 493:(2019), pp. 78-87. [10.1016/j.fluid.2019.04.011]

Availability:

This version is available at: 11583/2965630 since: 2022-06-01T18:59:25Z

Publisher:

Elsevier B.V.

Published

DOI:10.1016/j.fluid.2019.04.011

Terms of use:

This article is made available under terms and conditions as specified in the corresponding bibliographic description in the repository

Publisher copyright

Elsevier postprint/Author's Accepted Manuscript

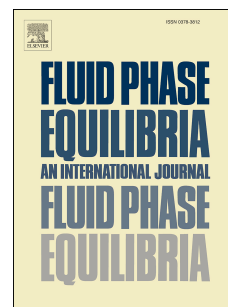
© 2019. This manuscript version is made available under the CC-BY-NC-ND 4.0 license
<http://creativecommons.org/licenses/by-nc-nd/4.0/>. The final authenticated version is available online at:
<http://dx.doi.org/10.1016/j.fluid.2019.04.011>

(Article begins on next page)

Accepted Manuscript

Solubility of three natural compounds with insecticidal activity in supercritical carbon dioxide: Experimental measurements and predictive modeling with the GC-EoS

Hernán Mazzei, Leonardo Ortega, Alfonsina E. Andreatta, Nicolás A. Gañán



PII: S0378-3812(19)30168-2

DOI: <https://doi.org/10.1016/j.fluid.2019.04.011>

Reference: FLUID 12156

To appear in: *Fluid Phase Equilibria*

Received Date: 10 December 2018

Revised Date: 9 April 2019

Accepted Date: 9 April 2019

Please cite this article as: Herná. Mazzei, L. Ortega, A.E. Andreatta, Nicolás.A. Gañán, Solubility of three natural compounds with insecticidal activity in supercritical carbon dioxide: Experimental measurements and predictive modeling with the GC-EoS, *Fluid Phase Equilibria* (2019), doi: <https://doi.org/10.1016/j.fluid.2019.04.011>.

This is a PDF file of an unedited manuscript that has been accepted for publication. As a service to our customers we are providing this early version of the manuscript. The manuscript will undergo copyediting, typesetting, and review of the resulting proof before it is published in its final form. Please note that during the production process errors may be discovered which could affect the content, and all legal disclaimers that apply to the journal pertain.

**Solubility of three natural compounds with insecticidal activity in
supercritical carbon dioxide: Experimental measurements and
predictive modeling with the GC-EoS**

Hernán Mazzei^a, Leonardo Ortega^a, Alfonsina E. Andreatta^b, Nicolás A. Gañán^{a,c,*}

^a *Universidad Nacional de Córdoba, Facultad de Ciencias Exactas, Físicas y Naturales,
Instituto de Ciencia y Tecnología de los Alimentos (ICTA–FCEFyN–UNC). Av. Vélez
Sarsfield 1611, X5016GCA, Córdoba, Argentina.*

^b *Universidad Tecnológica Nacional (UTN-Regional San Francisco), CONICET. Av. de
la Universidad 501, San Francisco, Argentina.*

^c *Instituto de Investigación y Desarrollo en Ingeniería de Procesos y Química Aplicada
(IPQA–UNC–CONICET), Av. Vélez Sarsfield 1611, X5016GCA, Córdoba, Argentina.*

^{*} *E-mail address: nicolas.ganan@unc.edu.ar*

ABSTRACT

In this work, the solubility of thymoquinone, *R*-(+)-pulegone and 1-octen-3-ol in supercritical CO₂ is determined in a range of conditions typical of supercritical fluid processes such as extraction, fractionation and impregnation. These compounds were selected based in their insecticidal activity which may enable to apply them as biopesticides. Solubility was measured using a semicontinuos method in the temperature range of 45–65°C and pressure of 8–12 MPa, at a CO₂ flowrate of 0.05–0.10 g/min, which was verified to be low enough to ensure saturation. Solubilities were predicted using the Group Contribution Equation of State (GC-EoS) and compared to the experimental results, with a good agreement. Consistency of the data was tested using the density-based Chrastil equation.

Key words: solubility, thymoquinone, *R*-(+)-pulegone, 1-octen-3-ol, supercritical carbon dioxide, GC-EoS.

1. Introduction

Essential oils and many of their volatile components show a wide range of bioactive properties, and therefore they are currently used in cosmetic, perfume, sanitary and oral care products, as well as in agronomic industry, as food preservatives and additives, and in pharmaceutical formulations [1], besides their use in traditional medicine since ancient times.

In this work, the solubility of three selected bioactive compounds in supercritical CO₂ (scCO₂), namely thymoquinone, *R*-(+)-pulegone and 1-octen-3-ol, naturally occurring in several essential oils, is presented. The chemical structures of these compounds are shown in **Table 1**. Thymoquinone is extracted from several plants, such as *Nigella sativa* (black cumin) [2], *Origanum vulgare* L. [3], *Monarda didyma* (scarlet bee balm), *Monarda fistulosa* (wild bergamot) [4], *Thymus pulegioides*, *Thymus serpyllum*, *Thymus vulgaris*, *Satureja hortensis*, *Satureja montana*, *Eupatorium cannabinum* and *Juniperus communis* [5], among others. This compound is claimed to show antioxidant, anti-inflammatory, anticancer, antimicrobial, hepatoprotective, immunomodulatory, and antiparasitic activities [6][7][8], which explains the interest of its recovery from herbs. *R*-(+)-pulegone is a monoterpene ketone present in the essential oil of many mint species, sometimes in a very high percentage [9]. For example, it is the major constituent of *Mentha pulegium* [10], *Minthostachys verticillata* [11] and, in minor concentration, is also present in peppermint oil (*Mentha piperita*) [9] and *Zuccagnia punctata* [12], among others. Toxicity effects of pulgone have been observed in mice, rats and humans because it is oxidized by cytochrome P450 to reactive metabolites such as menthofuran [13][14]. Consequently, pulgone is subject to several regulations as flavouring agent by the European Parliament and limitations in its use as cosmetic ingredient [13]. Finally, 1-

1 octen-3-ol (also known as “mushroom alcohol”) is a volatile compound present in
2 several plant species such as *Lantana camara* [15], *Premna integrifolia* [16], *Epilobium*
3 *parviflorum* [17], in essential oils extracted with scCO₂ from rosemary [18] and lavender
4 [19], etc. It is also used as a spoilage indicator in stored cereals because it is one of the
5 most important flavor components produced by mushrooms [20].

6 Besides other specific properties, these compounds have been selected in this work
7 mainly due to their potential use as biopesticides. With the aim to reduce the use of
8 chemical insecticides and establish limits on the application of synthetic pesticides
9 (organophosphates, chlorates and carbamates) to agricultural products, biopesticides
10 appear as “green” alternatives, with low impact on human health and environment and
11 high selectivity [21]. Although the direct replacement of synthetic pesticides by
12 biopesticides on field faces important technological and economical barriers, there are
13 several other promising applications for this kind of compounds [22], such as pest
14 control in confined places (for example, silos and other storing places of grains and
15 derivative products) and active food packaging materials. Moreover, the increasing
16 restrictions to the use of synthetic pesticides promotes the development of integrated pest
17 management (IPM) systems, combining the effect of different physical, chemical and
18 biological agents for pest control, in which biopesticides can find application
19 opportunities [23]. Finally, the increasing market of “organic” or “bio” food represents
20 another interesting niche of application. Insecticidal activity of thymoquinone and *R*-(+)-
21 pulegone (alone and in combination), as well as 1-octen-3-ol, against the corn weevil
22 (*Sitophilus zeamais*) has been reported by Herrera et al. [24]. Abdelli et al. [10] present a
23 valorization of pulegone-rich *M. pulegium* essential oil as an effective natural bio-agent
24 with antimicrobial and insecticidal properties. Rossi et al. [11] have reported insecticidal
25 and repellent activity to *Musca domestica* with *M. verticillata* essential oil and pulegone.

1 1-Octen-3-ol has a broad spectrum of action against different genera of fungi [25]
2 because it plays a role as a self-inhibitor [26], blocking the germination process. Owing
3 to this, 1-octen-3-ol, as well as other fungal volatile compounds, have been proposed as
4 protecting agents against pathogenic species in sustainable agriculture [27] and for
5 preventing post-harvest fungal growth in the food industry [28].

6 Several studies have been reported in the literature regarding supercritical processing of
7 these compounds, or extracts containing them. For example, Goñi et al. [29] have
8 recently studied the scCO₂-assisted impregnation of low density polyethylene films with
9 thymoquinone and *R*-(+)-pulegone, for developing active packaging materials or delivery
10 devices for protecting seeds, kernels and derivatives from insect pests, showing the
11 importance of the fluid phase concentration on impregnation yield and kinetics. Moreover,
12 Sovová et al. [4] have investigated the scCO₂ extraction of thymoquinone from *M.*
13 *didyma* and *M. fistulosa*, concluding that this procedure yields extracts with higher
14 thymoquinone content than conventional hydrodistillation. The same conclusion has
15 been pointed out by Grosso et al. [30] for *S. montana* extracts, and by Solati et al. [31]
16 for *N. sativa* seed oil. Gurganova et al. [32] have studied the recovery of thymoquinone
17 from *N. sativa* seed oil by continuous scCO₂ extraction, using a mixture of
18 thymoquinone and rapeseed oil as model system. For this purpose, they have obtained
19 dynamic and static equilibrium data of this system [33], as well as some binary data for
20 the [thymoquinone + CO₂] system near the critical point of the mixture at 50°C [34].
21 Finally, scCO₂ countercurrent fractionation can also be applied as an alternative
22 methodology to reduce the content of pulegone and other related ketones in mint
23 essential oils, as well as to recover active compounds from dementholized mint oils, as
24 demonstrated in a previous work [35]. In this sense, Madzimbamuto et al. [36] have
25 studied the scCO₂ fractionation of buchu oil in order to remove or reduce its naturally

high and undesired percentage of pulegone, reporting high pressure binary equilibrium data of its main components and CO₂.

The knowledge of the solubility of the compounds of interest in scCO₂ constitutes a key parameter in supercritical processes, as it determines the amount of fluid required or the highest concentration that can be obtained in the fluid phase in an impregnation, particle formation, fractionation or extraction system. Based on this, in the present work the solubility of thymoquinone, *R*-(+)-pulegone and 1-octen-3-ol in scCO₂ was measured using a semicontinuous method at different temperature and pressure conditions, which are representative of the typical operation ranges, and results were modeled using the Group Contribution Equation of State (GC-EoS) [37], with the objective of providing useful data for the design and optimization of supercritical processes. This model has been successfully applied in previous works concerning fractionation of essential oils [35][38]. It has proven a very good capability for predictive phase equilibrium calculations of asymmetric mixtures at high pressure conditions. Besides, it allows calculation of other equilibrium properties which are useful for process design (fugacity coefficients, phase envelopes, etc.) which cannot be obtained, for example, by empirical or semi-empirical solubility methods.

2. Materials and methods

2.1. Materials

The solutes and solvents used in this work, including their purity, source, CAS number, molecular weight, normal melting point and chemical structure, are reported in **Table 1**. Food grade ethanol (96% v/v, Porta Hnos., Argentina) was used for cleaning the

experimental equipment. All these chemicals were used directly without further purification.

2.2. Experimental setup and procedure

Solubility measurements were performed using a dynamic or “gas saturation” method in a high pressure equipment schematically represented in **Fig. 1**, and described in detail in a previous work [35]. In brief, it consists in a stainless steel column (inner diameter: 0.9 cm, height: 30 cm) connected to a CO₂ delivery system. The column is externally heated by an aluminium jacket and a set of electrical clamp resistances connected to a PID temperature controller (DH 101, Dhacel, Argentina), with a precision of ± 0.1 °C. Pressure is measured with a pressure transducer (CS-PT300 Xian Chinastar M&C Ltd., China) within a range of ± 0.1 MPa.

In a typical measurement, the column is filled with 0.5 mm diameter glass beads mixed with the compound whose solubility is to be determined (~1 g in all cases). Glass wool filters are placed at the column inlet and outlet in order to support the glass beads and avoid entrainment of solute droplets or particles. After loading the column, it is slowly filled with CO₂ directly from the tank, until reaching the saturation pressure at the prevailing ambient conditions. CO₂ is allowed to flow by 20-30 min in order to remove the air initially present in the column. At this point, the heating system is turned on and the system is allowed to equilibrate at the desired operation temperature. Meanwhile, CO₂ from the tank is cooled to approx. 1°C in a coil immersed in an ice-water bath, and stored as a liquid in the pressure generator cylinder (HiP, USA). Once the temperature is stable, CO₂ is fed from the pressure generator to the column until reaching the desired operation pressure. Immediately before entering the column, CO₂ goes through a pre-

1 heating coil kept at the desired operation temperature. This operation is performed
2 slowly, and several adjustments may be necessary until the system conditions are in
3 equilibrium. After a static period of 2 h, during which the system is allowed to
4 equilibrate with all valves closed, the dynamic extraction step is performed by opening
5 slowly the inlet and outlet valves and keeping a constant flow of CO₂. The flow rate is
6 adjusted to the desired value and controlled at regular intervals by a bubble gas meter.
7 The outlet stream is depressurized in a micrometering valve (Swagelok, USA) heated by
8 an electrical tape in order to avoid condensation or deposition of solid particles due to the
9 rapid cooling of CO₂. After some minutes of stabilization, the solute trap is connected to
10 the outlet valve. In the case of *R*-(+)-pulegone and 1-octen-3-ol, this trap consisted of a
11 glass U-tube partially filled with metallic mesh and immersed in a -40°C silicone oil
12 cooling bath (RE-107, Lauda, Germany). U-tubes are thoroughly cleaned with ethanol
13 and compressed air, and dried in an oven at 115°C before each use. The amount of solute
14 recovered in the trap during a certain period is determined gravimetrically by measuring
15 the mass increase of the trap in an analytical balance (Ohaus Adventurer Pro, New
16 Jersey, USA, $d=0.1$ mg). The corresponding amount of CO₂ is determined volumetrically
17 by the bubble gas meter at ambient temperature, pressure and humidity conditions. In the
18 case of thymoquinone, due to the difficulties in recovering this solid compound in the U-
19 tubes, the trap was replaced by a glass flask filled with a certain volume of 2-propanol
20 (previously saturated with CO₂). The geometry of this flask allows the CO₂ stream to
21 bubble from the bottom into the solvent, which dissolves the extracted solute. The
22 stripped gas is measured in the bubble flow meter. During measurements, the flask is
23 immersed into the cooling bath in order to minimize solvent evaporation. After solute
24 collection, the solution is analyzed in a UV-visible spectrophotometer (Lambda 25,
25 Perkin-Elmer, USA) at 252 nm, and the amount of solute is calculated from a calibration

curve. From this information, the solubility of each compound in scCO₂ was calculated as mole fraction (y_2). The experimental procedure was validated by reproduction of reported solubility data of *D*-limonene (for the U-tube trap) and diphenylamine (for the solvent trap), as will be shown in the Results and discussion section.

Solubility was measured at 45, 55 and 65°C and in a pressure range of approx. 8.0–12.0 MPa for *R*-(+)-pulegone and 1-octen-3-ol, which are typical conditions in supercritical CO₂ processes. In the case of thymoquinone, as its melting temperature is about 45°C [39], solubility was measured at 50 and 60°C. Although a melting point depression induced by CO₂ might be expected, temperatures above this value were selected in order to ensure liquid-fluid equilibrium conditions. Measurements were performed at increasing pressure and constant temperature, and each isotherm was determined by duplicate. Some points were also replicated independently. Therefore, all measurements are reported as an average of 2 to 4 replicates.

In addition, the optimal CO₂ flow rate was determined, in order to ensure that the outlet fluid stream is saturated with solute. In fact, if the flow rate is too high, thermodynamic equilibrium may not be achieved, and the solubility underestimated. Therefore, preliminary measurements were performed using *D*-limonene in order to determine a flow rate value (or range) where the observed solubility is maximum.

3. Thermodynamic modeling

3.1. GC-EOS model

Modeling of the binary solubility of the different compounds in scCO₂ was performed using the Group Contribution Equation of State (GC-EoS) [37]. This model is based in

the calculation of the Helmholtz free energy considering two contributions to non-ideality: a free-volume or repulsive term (calculated from molecular properties) and an attractive term (calculated using a group contribution approach). The model equations are detailed in **Appendix A**. The GC-EoS model has been successfully applied to the calculation of high pressure phase equilibria of a broad range of compounds using a limited number of functional groups and binary interaction parameters.

The critical properties and the group contribution structure of the studied compounds are presented in **Tables 2** and **3**, respectively. Except for CO₂, the critical temperatures and pressures were estimated using the group contribution method of Joback [40]. CO₂ critical properties, as well as its density at different temperature and pressure conditions, were taken from the NIST Chemistry Webbook database [41]. The critical diameter (d_c) of the pure compounds was adjusted from a vapor pressure point. The pure group, binary interaction and binary non-randomness parameters used in this model are presented in **Tables 4–6**. The most recent available version of the GC-EoS parameter matrix was used [42]. For the correct representation of pulegone, an olefinic group $>C=C<$ was necessary, which is not defined in the current parameter matrix. Instead of defining a new group, the existing $>C=CH-$ group and its corresponding set of parameters were used, modifying only the q parameter value (number of surface segments) by subtracting the contribution of one H atom. This approach has been previously applied in similar cases [35][38]. In the case of the binary interaction parameters between the ketone group and the olefinic groups, not available in the revised matrix, they were taken from our own previous adjustments [38]. The carbonyl groups in thymoquinone were represented using the $cyC=O$ group previously defined by Barrera et al. [43].

Calculations were performed in each case by solving a multiphase flash at fixed temperature and pressure with the subroutine GCTHREE [44] in a Fortran environment,

and were completely predictive, as no information from our experimental results was used for parameter adjustment. The model deviation was calculated in terms of the percent average relative deviation (ARD%), defined according to **Eq. 1**.

$$ARD\% = \frac{1}{N} \left(\sum_{i=1}^N \frac{|y_2^{calc} - y_2^{exp}|}{y_2^{exp}} \right) \times 100 \quad (1)$$

where N is the number of experimental data points, and y_2^{calc} and y_2^{exp} represent the calculated and experimental solubility (in mole fraction).

3.2. Chrastil equation

The well known density-based equation of Chrastil [45] adapted to liquid solutes was used as a test for checking the consistency of the data. This model correlates the solubility of a substance (S , in kg/m^3) with the pure CO_2 density and temperature, according to Eq. 2.

$$S = \rho^k e^{\left(\frac{a}{T} + b\right)} \quad (2)$$

where ρ is in kg/m^3 , T in K, and k , a and b are constant parameters. This equation can be rewritten in terms of the solute mass fraction (Y), according to Eq. 3.

$$\ln Y = (k - 1) \ln \rho + \frac{a}{T} + b \quad (3)$$

According to this expression, a plot of $\ln Y$ vs. $\ln \rho$ should be linear. The equation parameters were fitted by minimizing the deviation with the experimental data, calculated as $ARD\%$.

4. Results and discussion

As previously mentioned, the dynamic method was validated by reproduction of solubility data of *D*-limonene and diphenylamine in $scCO_2$ reported in the literature. These preliminary measurements involved the determination of the flow rate required for the saturation of the CO_2 stream in the extraction column. For that purpose, several runs were performed at fixed temperature and pressure conditions and varying the CO_2 flow rate, and the mole fraction of *D*-limonene in the fluid phase was quantified. **Fig. 2** shows results obtained at $60^\circ C$ and 8.2 MPa. As can be seen, the observed values are nearly constant below a flow rate of approx. 0.11 g/min, and decrease at higher rates, indicating that equilibrium is not achieved above this value, due to mass transfer limitations. From this information, all measurements in this work were performed at CO_2 flow rates within the range of 0.05–0.10 g/min. It has to be noted that the maximum saturation flow rate may depend on the CO_2 /substrate ratio inside the extractor, and therefore change with the loaded amount and with CO_2 density. In this case, considering the initial loading of 1 g of substrate, the cell volume and the temperature and pressure conditions tested, this ratio was in the range of 1.2 to 3.1 g/g in all experiments.

Table 7 shows the solubility values of *D*-limonene in $scCO_2$ obtained in this work using the gravimetric method at different temperature and pressure conditions, which are graphically compared to the values reported by other authors [46][47][48][49][50] in **Fig. 3**. Similarly, **Table 8** shows the solubility of diphenylamine in $scCO_2$ obtained in this

work with both the spectrophotometric and the gravimetric methods, compared with literature data [51] in **Fig. 4**. A good agreement between our data and the values from the literature is observed, taking into account the dispersion of the data, especially at lower pressure values. Note that these data have been obtained using different methods: Akgün et al. [46] applied a static method with chromatographic analysis of both phases; Sovová et al. [47] used a dynamic method with gravimetric quantification in a cooled U-tube; whereas Chang and Chen [48] determined the equilibrium compositions from density data measured in a densimeter with recirculation. In the case of Leeke et al. [49], a high pressure cell with recirculation and sampling was used for equilibrium measurements, while Matos et al. [50] determined the limonene concentration in the gas phase gravimetrically in a static high pressure cell.

Table 9 shows the experimental solubility values for thymoquinone at 50 and 60°C, as well as the GC-EoS predictive calculations. Results are graphically presented in **Fig. 5(a)**. As can be seen, a good agreement is observed between the GC-EoS predictions and the experimental values (ARD% of 20.8 and 13.8, at 50 and 60°C, respectively). Solubility increases about one order of magnitude in the studied pressure range, from approx. 10^{-4} to 10^{-3} (mole fraction). The occurrence of a “cross-over” point, where the temperature dependence of the solubility inverts, can also be noticed at a pressure value between 8.5 and 9.0 MPa, correctly predicted by the model. **Fig. 5(b)** shows the solubility values as a function of pure CO₂ density, as well as the correlations using the equation of Chrastil. A very good linear behavior is observed, with both isotherms overlapping, indicating that the Chrastil parameters are practically independent of temperature for this compound. There are few data in the literature concerning this particular system. Gurganova et al. [34] have determined the critical pressure of the [CO₂ + thymoquinone] mixture at 50°C by direct observation in a sapphire cell, being approx.

10.3 MPa. Although our data show a two-fold increase in solubility from 10.0 to 10.5 MPa at this temperature, we cannot ascertain that this corresponds to the critical point. Although the GC-EoS model correctly represents the solubility behavior below this pressure, it predicts biphasic conditions above this limit. These authors have also reported dynamic and static solubility data of thymoquinone in near-critical and supercritical CO₂ [33]. Their interest was to study the fractionation of thymoquinone from black cumin seed oil by scCO₂ extraction, and therefore they used a mixture of thymoquinone and rapeseed oil as model system, instead of pure thymoquinone. Although they claim that rapeseed oil solubility in CO₂ is negligible at the tested conditions, the fact that measurements are performed on a ternary system, and not a binary one, has important effects on the observed phase equilibrium. On the one hand, they report a marked dependence of solubility on the concentration of thymoquinone in the liquid feed. On the other, they observe solubility values of $0.7\text{--}5.4 \times 10^{-5}$ (mole fraction), at 28 and 38°C and pressures as high as 12 MPa. This indicates that the presence of the rapeseed oil, although practically not extracted in the supercritical phase, extends the heterogeneous region to higher pressure levels and yields even lower solubilities, with respect to the binary system. The difference between binary and multicomponent solubilities, which can be significant, has been previously pointed out by the authors for other terpenic mixtures [38].

The experimental and predicted solubility values of *R*-(+)-pulegone in sCO₂ at 45, 55 and 65°C are presented in **Table 10** and **Fig. 6(a)**. In this case, an exponential increase of solubility with pressure can be seen, as well as an increase of the heterogeneous region limits to higher pressure levels when increasing the temperature. The one order of magnitude increase observed at the highest pressure values, especially at 45 and 55°C, although typical in liquid-fluid equilibria near the critical region of the mixture, may also

1 indicate the occurrence of a single phase (complete miscibility). In order to check this
2 hypothesis, mass balances were performed in order to estimate the global concentration
3 inside the extractor column at these conditions (considering the amounts of pulegone
4 extracted in previous measurements and the losses during system stabilization), which
5 was found to be about the same order of magnitude of the observed solubility values,
6 although somewhat higher (0.02-0.03, mole fraction). Madzimbamuto et al. [36] have
7 reported high pressure equilibrium data for the [CO₂ + pulegone] system at various
8 temperatures (from 35 to 75°C). Although they present mainly bubble points and the gas-
9 phase data are scarce, their results suggest that the critical pressure of the mixture is near
10 9.5 MPa at 45°C, which is in agreement with our observations. At 55°C, the critical
11 pressure seems to be near 11.5 MPa and therefore it seems probable that we have
12 measured a single phase at 10.5 MPa. At 65°C, they observe that the critical pressure is
13 around 13.5 MPa, therefore our own measurements correspond entirely to gas-phase
14 solubilities. Although the GC-EoS model correctly describes the solubility behavior,
15 higher deviations are observed for this compound (ARD% up to 43.9%). These
16 differences, which increase at higher pressure, can be a consequence of the errors in the
17 prediction of equilibrium pressures in the near-critical region of the mixture. In this
18 sense, the effect of CO₂ density starts to override the effect of solute vapor pressure and
19 the solubilities become higher at lower temperatures. **Fig. 6(b)** suggests a significant
20 deviation from the expected linear dependence between the logarithm of the solubility
21 and the logarithm of CO₂ density, especially at 45°C, which may be due to experimental
22 errors near the critical point of the mixture or to the above-mentioned possibility of
23 having single phase conditions at the highest tested pressure. A temperature-dependence
24 of Chrastil parameters is also observed, as the isotherms present different slope and
25 intercept.

Finally, **Table 11** and **Fig. 7(a)** show the experimental and calculated solubility values for 1-octen-3-ol at 45, 55 and 65°C. The same one order of magnitude exponential increase of solubility with pressure is observed from 8 to 11 MPa (from approx. 10^{-3} to 10^{-2}). Globally, GC-EoS predictions are in good agreement with the observed behavior at 45 and 55°C (showing ARD% values of 7.3 and 18.1%), with higher deviations at 65°C (31.5%). It can also be noticed that the experimental solubility decreases with temperature at a given pressure in the whole studied range, although the model predicts the occurrence of “cross-over” points. Within the studied pressure range, no sharp increase of solubility is observed (as was the case for *R*-(+)-pulegone), indicating that measurements were taken relatively far below the critical point of the mixture. This extension of the heterogeneous region limits to higher pressure levels could be due to association effects which may be important in this alcohol. **Fig. 7(b)** indicates a good correlation between solubility and CO₂ density at the three studied temperatures. A certain temperature-dependence of the Chrastil parameters can also be observed for this compound. Although there are other studies in the literature regarding high pressure equilibrium of different C₈ alcohols and CO₂ [52], to the best of our knowledge, this is the first report of 1-octen-3-ol solubility data in scCO₂.

5. Conclusions

The solubility of thymoquinone, *R*-(+)-pulegone and 1-octen-3-ol in supercritical carbon dioxide were determined experimentally using a semicontinuous method in the temperature range of 45–65°C and a pressure range of approx. 8–12 MPa. The equation of Chrastil, used to test the consistency of the data, showed good results, with a temperature-dependence of the Chrastil parameters for *R*-(+)-pulegone and 1-octen-3-ol.

The GC-EoS model was used to predict the behavior of the three studied systems, achieving a good representation of the solubility conditions, though deviations tend to increase towards the critical region of the mixtures.

ACKNOWLEDGMENTS

The authors gratefully acknowledge the financial support of Consejo Nacional de Investigaciones Científicas y Técnicas (CONICET, Argentina), Agencia Nacional de Promoción Científica y Técnica (ANPCyT, Argentina), Secretaría de Ciencia y Técnica (Universidad Nacional de Córdoba, Argentina) and Universidad Tecnológica Nacional (UTN-Regional San Francisco, Argentina).

REFERENCES

- [1] F. Bakkali, S. Averbeck, D. Averbeck, M. Idaomar, Food Chem. Toxicol. 46 (2008) 446–475.
- [2] C. Detremmerie, P.M. Vanhoutte, S. Leung, Acta Pharm. Sin. B 7 (2017) 401–408.
- [3] B. Lukas, C. Schmiderer, J. Novak, Phytochemistry 119 (2015) 32–40.
- [4] H. Sovová, M. Sajfrtova, M. Topiar, J. Supercrit. Fluids 105 (2015) 29–34.
- [5] J. Taborsky, M. Kunt, P. Kloucek, J. Lachman, V. Zeleny, L. Kokoska, Cent. Eur. J. Chem. 10 (2012) 1899–1906.
- [6] C.C. Woo, A.P. Kumar, G. Sethi, K.H.B. Tan, Biochem. Pharmacol. 83 (2012) 443–451.
- [7] B.H. Ali, G. Blunden, Phyther. Res. 17 (2003) 299–305.

- 1 [8] S. Darakhshan, A. Bidmeshki Pour, A. Hosseinzadeh Colagar, S. Sisakhtnezhad,
2 Pharmacol. Res. 95 (2015) 138–158.
- 3 [9] K. Skalicka-Woźniak, M. Walasek, Phytochem. Lett. 10 (2014) xciv–xcviii.
- 4 [10] M. Abdelli, H. Moghrani, A. Aboun, R. Maachi, Ind. Crops Prod. 94 (2016) 197–
5 205.
- 6 [11] Y.E. Rossi, L. Canavoso, S.M. Palacios, Fitoterapia 83 (2012) 336–342.
- 7 [12] S.L. Álvarez, A. Cortadi, M.A. Juárez, E. Petenatti, F. Tomi, J. Casanova, C.M.
8 van Baren, S. Zacchino, R. Vila, Phytochem. Lett. 5 (2012) 194–199.
- 9 [13] B. Nair, Int. J. Toxicol. 20 (2001) 61–73.
- 10 [14] S.D. Nelson, R.H. McClanahan, D. Thomassen, W. Perry Gordon, N. Knebel,
11 Xenobiotica 22 (1992) 1157–1164.
- 12 [15] M. Khan, A. Mahmood, H.Z. Alkathlan, Arab. J. Chem. 9 (2016) 764–774.
- 13 [16] A. Rahman, Z. Sultana Shanta, M.A. Rashid, T. Parvin, S. Afrin, M. Khodeza
14 Khatun, M.A. Sattar, Arab. J. Chem. 9 (2016) S475–S479.
- 15 [17] T. Bajer, D. Šilha, K. Ventura, P. Bajerová, Ind. Crops Prod. 100 (2017) 95–105.
- 16 [18] E.M. Bittencourt Dutra de Sousa, V.A. Toussaint, A. Shariati, L.J. Florusse, O.
17 Chiavone-Filho, M.A.A. Meireles, C.J. Peters, Fluid Phase Equilib. 428 (2016) 32–
18 37.
- 19 [19] L.T. Danh, N.D.A. Triet, L.T.N. Han, J. Zhao, R. Mammucari, N. Foster, J.
20 Supercrit. Fluids 70 (2012) 27–34.
- 21 [20] D. Tuma, R.N. Sinha, W.E. Muir, D. Abramson, Int. J. Food Microbiol. 8 (1989)
22 103–119.
- 23 [21] C. Regnault-Roger, C. Vincent, J.T. Arnason, Annu. Rev. Entomol. 57 (2012)
24 405–424.
- 25 [22] M.B. Isman, S. Miresmailli, C. Machial. Phytochem. Rev. 11 (2011) 197–204.

- 1 [23] D. Chandler, A.S. Bailey, G.M. Tatchell, G. Davidson, J. Greaves, W.P. Grant.
2 Phil. Trans. R. Soc. B 336 (2011) 1987-1998.
- 3 [24] J.M. Herrera, M.P. Zunino, J.S. Dambolena, R.P. Pizzolitto, N.A. Gañan, E.I.
4 Lucini, J.A. Zygodlo, Ind. Crops Prod. 70 (2015) 435-442.
- 5 [25] G.S. Chitarra, T. Abee, F.M. Rombouts, M.A. Posthumus, J. Dijksterhuis, Appl.
6 Environ. Microbiol. 70 (2004) 2823-9.
- 7 [26] G.S. Chitarra, T. Abee, F.M. Rombouts, J. Dijksterhuis, FEMS Microbiol. Ecol. 54
8 (2005) 67-75.
- 9 [27] C.N. Kanchiswami, M. Malnoy, M.E. Maffei, Trends Plant Sci. 20 (2015) 206-
10 211.
- 11 [28] S.U. Morath, R. Hung, J.W. Bennett, Fungal Biol. Rev. 26 (2012) 73-83.
- 12 [29] M.L. Goñi, N.A. Gañán, J.M. Herrera, M.C. Strumia, A.E. Andreatta, R.E. Martini,
13 J. Supercrit. Fluids 122 (2017) 18-26.
- 14 [30] C. Grosso, A.C. Figueiredo, J. Burillo, A.M. Mainar, J.S. Urieta, J.G. Barroso, J.A.
15 Coelho, A.M.F. Palávra, J. Sep. Sci. 32 (2009) 328-334.
- 16 [31] Z. Solati, B.S. Baharin, H. Bagheri, Ind. Crop Prod. 36 (2012) 519-523.
- 17 [32] K. Gurganova, P. Wawrzyniak, D. Kalembe, Inz. Ap. Chem. 49 (2010) 47-48.
- 18 [33] K. Gurganova, P. Wawrzyniak, Inz. Ap. Chem. 51 (2012) 320-321.
- 19 [34] K. Gurganova, R. Bogel-Lukasik, P. Wawrzyniak, Chem. Process Eng. 34 (2013)
20 387-392.
- 21 [35] N.A. Gañán, J.S. Dambolena, R.E. Martini, S.B. Bottini, J. Supercrit. Fluids 98
22 (2015) 1-11.
- 23 [36] T.F.N. Madzimbamuto, C.E. Schwarz, J.H. Knoetze, J. Supercrit. Fluids 107
24 (2016) 612-623.
- 25 [37] S. Skjold-Jorgensen, Ind. Eng. Chem. Res. 27 (1988) 110-118.

- [38] N.A. Gañán, E.A. Brignole, J. Supercrit. Fluids 58 (2011) 58–67.
- [39] S. Pagola, A. Benavente, A. Raschi, E. Romano, M.A.A. Molina, P.W. Stephens, AAPS PharmSciTech 5 (2004) 24–31.
- [40] B.E. Poling, J.M. Prausnitz, J.P. O’Connell, The Properties of Gases and Liquids (2001).
- [41] NIST Chemistry Webbook (2018). <https://webbook.nist.gov/chemistry/fluid/>
- [42] T. Fornari, Fluid Phase Equilibr. 262 (2007) 187–209.
- [43] M.F. Barrera-Vázquez, N.A. Gañán, L.R. Comini, R.E. Martini, S.B. Bottini, A.E. Andreatta, J. Supercrit. Fluids 125 (2017) 1–11.
- [44] M.L. Michelsen, Fluid Phase Equilibr. 9 (1982) 21–44.
- [45] J. Chrastil, J. Phys. Chem. 86 (1982) 3016–3021.
- [46] M. Akgün, N.A. Akgün, S. Dincer, J. Supercrit. Fluids 15 (1999) 117–125.
- [47] H. Sovová, R. Stateva, A.A. Galushko, J. Supercrit. Fluids 20 (2001) 113–129.
- [48] C.M.J. Chang, C.C. Chen, Fluid Phase Equilibr. 163 (1999) 119–126.
- [49] G. Leeke, R. Santos, M.B. King, J. Chem. Eng. Data 46 (2001) 541–545.
- [50] H.A. Matos, E. Gomes de Acevedo, P.C. Simoes, M.T. Carrondo, M. Nunes da Ponte, Fluid Phase Equilibr. 52 (1989) 357–364.
- [51] Y.V. Tsekhanskaya, M.B. Iomtev, E.V. Mushkina, Zh. Fiz. Khim+ 36 (1962) 2187–2193.
- [52] F.C.v.N. Fourie, C.E. Schwarz, J.H. Knoetze, J. Supercrit. Fluids 47 (2008) 161–167.
- [53] G. Mansoori, N. Carnahan, K. Starling, T. Leeland, J. Chem. Phys. 54 (1971) 1523.

Appendix A. GC-EoS model equations.

The GC-EoS model computes the residual Helmholtz energy (A^{res}) by two additive contributions: a repulsive or free volume term (A^{fv}) and an attractive term accounting for intermolecular forces (A^{att}):

$$A^{res} = A^{fv} + A^{att} \quad (A.1)$$

The free volume term is modeled using a Carnahan-Starling type hard sphere expression, developed by Mansoori and Leland [53]:

$$\frac{A^{fv}}{RT} = 3 \left(\frac{\lambda_1 \lambda_2}{\lambda_3} \right) (Y - 1) + \left(\frac{\lambda_2^3}{\lambda_3^2} \right) (-Y + Y^2 - \ln Y) + n \ln Y \quad (A.2)$$

where:

$$Y = \left(1 - \frac{\pi \lambda_3}{6V} \right)^{-1} \quad (A.3)$$

$$\lambda_k = \sum_i^{NC} n_i d_i^k \quad (A.4)$$

V is the total volume, NC the number of components in the mixture, n_i is the number of moles of component i , n is the total mole number and d_i is the temperature dependent hard sphere diameter of each component, calculated as:

$$d_i = 1.065655d_{c,i} \left[1 - 0.12 \exp\left(\frac{-2T_{c,i}}{3T}\right) \right] \quad (\text{A.5})$$

where $d_{c,i}$ is the pure component critical hard sphere diameter. This parameter can be fitted to a vapor pressure point, or calculated from the pure compound critical properties (T_c and P_c) as:

$$d_{c,i} = \left(\frac{0.08943RT_{c,i}}{P_{c,i}} \right)^{1/3} \quad (\text{A.6})$$

The attractive term is a group contribution version of a NRTL type expression with density dependent mixing rules:

$$\frac{A^{att}}{RT} = -\frac{z}{2} \sum_i^{NC} n_i \sum_j^{NG} v_j^i q_j \sum_k^{NG} (\theta_k g_{kj} \tilde{q} \tau_{kj} / RTV) / \sum_l^{NG} \theta_l \tau_{lj} \quad (\text{A.7})$$

where:

$$\theta_j = \left(\frac{q_j}{\tilde{q}} \right) \sum_i^{NC} n_i v_j^i \quad (\text{A.8})$$

$$\tilde{q} = \sum_i^{NC} n_i \sum_j^{NG} v_j^i q_j \quad (\text{A.9})$$

$$\tau_{ij} = \exp\left(\frac{\alpha_{ij} \Delta g_{ij} \tilde{q}}{RTV}\right) \quad (\text{A.10})$$

$$\Delta g_{ij} = g_{ij} - g_{jj} \quad (\text{A.11})$$

NG is the number of groups, z is the coordination number of any segment (set to 10), v_j^i is the number of groups of type j in molecule i , q_j is the number of surface segments assigned to group j , θ_k is the surface fraction of group k , \tilde{q} is the total number of surface segments, g_{ij} is the attraction energy parameter between groups i and j ($g_{ij} = g_{ji}$), and α_{ij} is the binary non-randomness parameter ($\alpha_{ij} \neq \alpha_{ji}$). The binary interaction parameters between unlike groups are calculated as:

$$g_{ij} = k_{ij}(g_{ii}g_{jj})^{1/2} \quad (k_{ij} = k_{ji}) \quad (\text{A.12})$$

with the following temperature dependences:

$$g_{jj} = g_{jj}^* \left[1 + g'_{jj} \left(\frac{T}{T_j^*} - 1 \right) + g''_{jj} \ln \left(\frac{T}{T_j^*} \right) \right] \quad (\text{A.13})$$

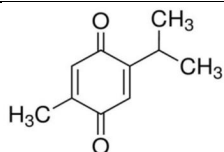
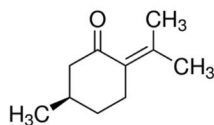
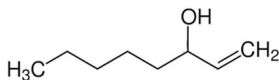
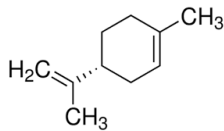
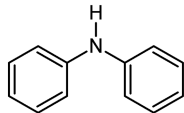
$$k_{ij} = k_{ij}^* \left[1 + k'_{ij} \ln \left(\frac{2T}{T_i^* + T_j^*} \right) \right] \quad (\text{A.14})$$

where g_{jj}^* is the interaction parameter for the pure group j at the reference temperature T_j^* .

The detailed description of this model can be found in the works by Skjold-Jørgensen [37].

TABLES

Table 1. Chemicals used in this work, including chemical structure, CAS number, purity, supplier, molecular weight (*MW*) and normal melting point of the solutes (*T_m*).

Compound	Chemical structure	CAS number	Purity (wt%) ^a	Source	<i>MW</i> (g/mol)	<i>T_m</i> (°C)
Thymoquinone		490-91-5	≥99	Sigma-Aldrich, Germany	164.2	45.1 ^b
<i>R</i> -(+)-Pulegone		89-82-7	≥97	Sigma-Aldrich, Germany	152.2	-25.1 ^c
1-Octen-3-ol		3391-86-4	≥98	Sigma-Aldrich, Germany	128.2	-49.7 ^c
<i>D</i> -Limonene		138-86-3	≥97	Sigma-Aldrich, Germany	136.2	-74.5 ^d
Diphenylamine		122-39-4	≥99	Sigma-Aldrich, Germany	169.2	52.9 ^e
CO ₂		124-38-9	≥99.99	Linde, Argentina	44.0	
2-propanol		67-63-0	≥99.5	Cicarelli, Argentina	60.1	

^a No previous purification was performed.

^b From literature [39]. Determined by differential thermal analysis (DTA) and differential scanning calorimetry (DSC). Standard uncertainty: $u(T) = 2.2^{\circ}\text{C}$.

^c Estimated by Joback's group contribution method [40].

^d From NIST Chemistry Webbook [41]. Measured in a freezing tube. Standard uncertainty: $u(T) = 0.15^{\circ}\text{C}$.

^e From NIST Chemistry Webbook [41]. Average of 21 values. Standard uncertainty: $u(T) = 2^{\circ}\text{C}$.

Table 2. Critical temperature (T_c), critical pressure (P_c) and critical diameter (d_c) of studied compounds

	T_c (°C)	P_c (MPa)	d_c (cm/mol)
CO ₂	31.1 ^a	7.38 ^a	3.129 ^c
Thymoquinone	289.4 ^b	3.93 ^b	5.904 ^c
<i>R</i> -(+)-pulegone	201.0 ^b	2.76 ^b	6.036 ^c
1-octen-3-ol	166.9 ^b	2.77 ^b	5.559 ^c

^a From NIST Webbook database [41].

^b Estimated by the Joback group contribution method [40].

^c Determined from a vapor pressure point.

Table 3. GC-EoS group structure of studied compounds

	thymoquinone	<i>R</i> -(+)-pulegone	1-octen-3-ol	CO ₂
CH ₃	3	3	1	-
CH ₂	-	-	4	-
CH	1	-	-	-
cyCH ₂	-	2	-	-
cyCH	-	1	-	-
CH ₂ =CH	-	-	1	-
C=CH	2	1 ^a	-	-
CHOH	-	-	1	-
CH ₂ C=O	-	1	-	-
cyC=O	2	-	-	-
CO ₂	-	-	-	1

^a Redefined as C=C

Table 4. Pure group parameters

	q	T	g	g'	g''
CH ₃	0.848	600	316910	-0.9274	0
CH ₂	0.540	600	356080	-0.8755	0
CH	0.228	600	356080	-0.8755	0
cyCH ₂	0.540	600	466550	-0.6062	0
cyCH	0.228	600	466550	-0.6328	0
CH ₂ =CH	1.176	600	337980	-0.6764	0
C=CH	0.676 ^a	600	546780	-1.0966	0
CHOH	0.908	512.6	1207500	-0.6441	0
CH ₂ C=O	1.180	600	888410	-0.7018	0
cyC=O	0.640	600	888410	-0.7018	0
CO ₂	1.261	304.2	531890	-0.5780	0

^a $q = 0.485$ in *R*-(+)-pulegone.

Table 5. Binary interaction parameters (k_{ij} above diagonal and k'_{ij} below diagonal)

	CH ₃	CH ₂	CH	cyCH ₂	cyCH	CH ₂ =CH	C=CH	CHOH	CH ₂ C=O	cyC=O	CO ₂
CH ₃	-	1.000	1.000	1.000	1.000	0.977	1.000	0.715	0.834	0.834	0.898
CH ₂	0.000	-	n.n.	n.n.	n.n.	0.977	n.n.	0.682	n.n.	n.n.	0.814
CH	0.000	n.n.	-	n.n.	n.n.	n.n.	1.000	n.n.	n.n.	0.834	0.814
cyCH ₂	0.000	n.n.	n.n.	-	1.000	n.n.	1.000	n.n.	0.870	n.n.	0.928
cyCH	0.000	n.n.	n.n.	0.000	-	n.n.	1.000	n.n.	0.870	n.n.	0.928
CH ₂ =CH	0.000	0.000	n.n.	n.n.	n.n.	-	n.n.	1.040	n.n.	n.n.	0.948
C=CH	0.000	n.n.	0.000	0.000	0.000	n.n.	-	n.n.	1.000	0.975	1.000
CHOH	0.000	0.000	n.n.	n.n.	n.n.	0.000	n.n.	-	n.n.	n.n.	0.785
CH ₂ C=O	0.084	n.n.	n.n.	0.097	0.097	n.n.	0.000	n.n.	-	n.n.	1.025
cyC=O	0.084	n.n.	0.084	n.n.	n.n.	n.n.	0.000	n.n.	n.n.	-	1.025
CO ₂	0.000	0.000	0.000	0.210	0.210	0.000	0.000	0.000	0.108	0.108	-

n.n.: not necessary for calculations

1 **Table 6.** Binary non-randomness parameters (α_{ij} above diagonal and α_{ji} below diagonal)

2

	CH ₃	CH ₂	CH	cyCH ₂	cyCH	CH ₂ =CH	C=CH	CHOH	CH ₂ C=O	cyC=O	CO ₂
CH ₃	-	0.000	0.000	0.000	0.000	0.000	0.000	1.471	0.854	0.854	4.683
CH ₂	0.000	-	n.n.	n.n.	n.n.	0.000	n.n.	1.471	n.n.	n.n.	4.683
CH	0.000	n.n.	-	n.n.	n.n.	n.n.	0.000	n.n.	n.n.	0.854	4.683
cyCH ₂	0.000	n.n.	n.n.	-	0.000	n.n.	0.000	n.n.	0.854	n.n.	0.000
cyCH	0.000	n.n.	n.n.	0.000	-	n.n.	0.000	n.n.	0.851	n.n.	0.000
CH ₂ =CH	0.000	0.000	n.n.	n.n.	n.n.	-	n.n.	0.000	n.n.	n.n.	0.000
C=CH	0.000	n.n.	0.000	0.000	0.000	n.n.	-	n.n.	0.000	0.000	0.000
CHOH	10.22	10.22	n.n.	n.n.	n.n.	0.000	n.n.	-	n.n.	n.n.	-1.180
CH ₂ C=O	5.146	n.n.	n.n.	5.146	5.146	n.n.	0.000	n.n.	-	n.n.	0.170
cyC=O	5.146	n.n.	5.146	n.n.	n.n.	n.n.	0.000	n.n.	n.n.	-	0.170
CO ₂	4.683	4.683	4.683	0.000	0.000	0.000	0.000	0.220	0.170	0.170	-

3 n.n.: not necessary for calculations

4

5

6

Table 7. Experimental solubility of liquid *D*-limonene in scCO₂ (y_2), given as mean value \pm standard deviation ($n = 2$).

T (°C)	P (MPa)	$y_2 (\times 10^3)$
50	7.6	3.13 ± 0.25
	8.2	3.43 ± 0.11
	9.3	6.77 ± 0.57
60	8.2	2.18 ± 0.17
	9.0	3.59 ± 0.03
	9.9	4.01 ± 0.63

Standard uncertainties are: $u(T) = \pm 0.1^\circ\text{C}$; $u(P) = \pm 0.1$ MPa; $u_r(y_2) = \pm 7.1\%$.

Table 8. Experimental solubility of solid diphenylamine in scCO₂ (y₂), given as mean value \pm standard deviation ($n = 2$).

T (°C)	P (MPa)	$y_2 (\times 10^3)$,	$y_2 (\times 10^3)$,
		gravimetric	spectrophotometric
32	8.5	1.41 ± 0.02	1.07 ± 0.01
	9.0	1.59 ± 0.11	1.45 ± 0.03
	10.0	2.77 ± 0.07	2.66 ± 0.10
37	8.2	1.74 ± 0.07	2.00 ± 0.10
	9.0	2.30 ± 0.03	2.34 ± 0.15
	10.0	3.14 ± 0.19	3.50 ± 0.22

Standard uncertainties are: $u(T) = 0.1^\circ\text{C}$; $u(P) = 0.1$ MPa; $u_r(y_2) = \pm 3.7\%$ (gravimetric); $u_r(y_2) = \pm 4.1\%$ (spectrophotometric).

Table 9. Experimental and calculated solubility of liquid thymoquinone (y_2) in scCO₂.

Experimental results are given as mean value \pm standard deviation ($n = 2-4$).

T (°C)	P (MPa)	$y_2^{\text{exp}} (\times 10^3)$	$y_2^{\text{calc}} (\times 10^3)$	$ARD\%$
50	8.0	0.27 ± 0.03	0.22	20.8
	8.5	0.40 ± 0.05	0.32	
	9.0	0.55 ± 0.04	0.48	
	9.5	0.75 ± 0.17	0.77	
	10.0	0.95 ± 0.22	1.31	
	10.5	1.74 ± 0.30	2.31	
60	8.0	0.33 ± 0.05	0.28	13.8
	8.5	0.41 ± 0.08	0.35	
	9.0	0.52 ± 0.03	0.45	
	9.5	0.55 ± 0.08	0.59	
	10.0	0.63 ± 0.07	0.79	
	10.5	1.18 ± 0.10	1.08	

Standard uncertainties are: $u(T) = 0.1^\circ\text{C}$; $u(P) = 0.1 \text{ MPa}$; $u_r(y_2^{\text{exp}}) = \pm 14\%$.

Table 10. Experimental and calculated solubility of liquid pulegone (y_2) in scCO_2 .Experimental results are given as mean value \pm standard deviation ($n = 2-4$).

T ($^{\circ}\text{C}$)	P (MPa)	$y_2^{\text{exp}} (\times 10^3)$	$y_2^{\text{calc}} (\times 10^3)$	$ARD\%$
45	8.0	0.87 ± 0.17	0.41	43.9
	8.5	1.15 ± 0.04	0.66	
	9.0	1.20 ± 0.45	1.26	
	9.5	12.31 ± 3.43	3.05	
55	8.0	0.58 ± 0.11	0.44	29.4
	8.5	0.52 ± 0.15	0.57	
	9.0	0.66 ± 0.16	0.77	
	9.5	1.07 ± 0.20	1.08	
	10.0	2.67 ± 0.05	1.59	
	10.5	14.10 ± 2.51	2.43	
65	8.0	0.56 ± 0.01	0.55	27.4
	9.0	0.47 ± 0.05	0.81	
	9.5	1.00 ± 0.07	1.00	
	10.0	1.37 ± 0.12	1.27	
	10.5	2.10 ± 0.14	1.64	
	11.0	5.71 ± 1.44	2.14	

Standard uncertainties are: $u(T) = 0.1^{\circ}\text{C}$; $u(P) = 0.1 \text{ MPa}$; $u_r(y_2) = \pm 16\%$.

Table 11. Experimental and calculated solubility of liquid 1-octen-3-ol (y_2) in scCO_2 .Experimental results are given as mean value \pm standard deviation ($n = 2-4$).

T ($^{\circ}\text{C}$)	P (MPa)	$y_2^{\text{exp}} (\times 10^3)$	$y_2^{\text{calc}} (\times 10^3)$	$ARD\%$
45	8.0	1.10 ± 0.09	0.99	7.3
	8.5	1.45 ± 0.49	1.43	
	9.0	2.86 ± 0.11	2.31	
	9.5	4.19 ± 0.12	4.04	
	10.0	6.17 ± 0.00	6.27	
55	8.0	0.88 ± 0.10	1.06	18.1
	8.5	1.12 ± 0.29	1.31	
	9.0	1.77 ± 0.90	1.64	
	9.5	2.09 ± 0.33	2.12	
	10.0	3.18 ± 0.52	2.81	
	10.5	7.46 ± 1.00	3.77	
65	8.0	0.73 ± 0.00	1.34	31.5
	9.0	1.36 ± 0.12	1.79	
	9.5	2.01 ± 0.15	2.11	
	10.0	2.43 ± 0.33	2.51	
	10.5	3.49 ± 0.62	3.02	
	11.0	7.82 ± 1.22	3.67	

Standard uncertainties are: $u(T) = 0.1^{\circ}\text{C}$; $u(P) = 0.1$ MPa; $u_r(y_2) = \pm 14\%$.

FIGURES

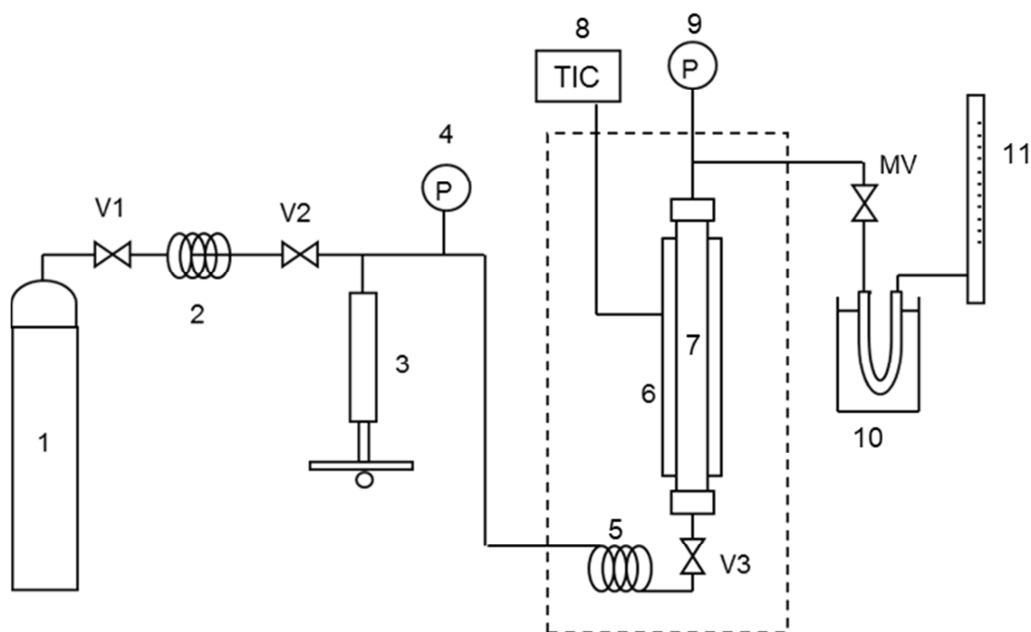


Figure 1. Experimental setup. (1) CO₂ reservoir; (2) cooling coil; (3) pressure generator; (4) manometer; (5) pre-heating coil; (6) heating jacket; (7) high pressure cell; (8) temperature controller; (9) pressure transducer; (10) cold trap; (11) bubble flow meter; (V) on-off valves; (MV) micrometering valve.

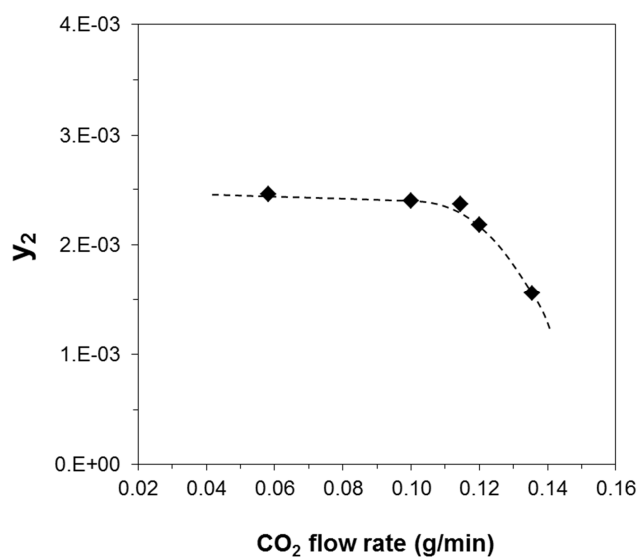


Figure 2. Mole fraction of liquid *D*-limonene in scCO_2 (y_2) as a function of CO_2 flow rate at $T = 60^\circ\text{C}$ and $P = 8.2$ MPa. Dotted line provided only for visual guidance.

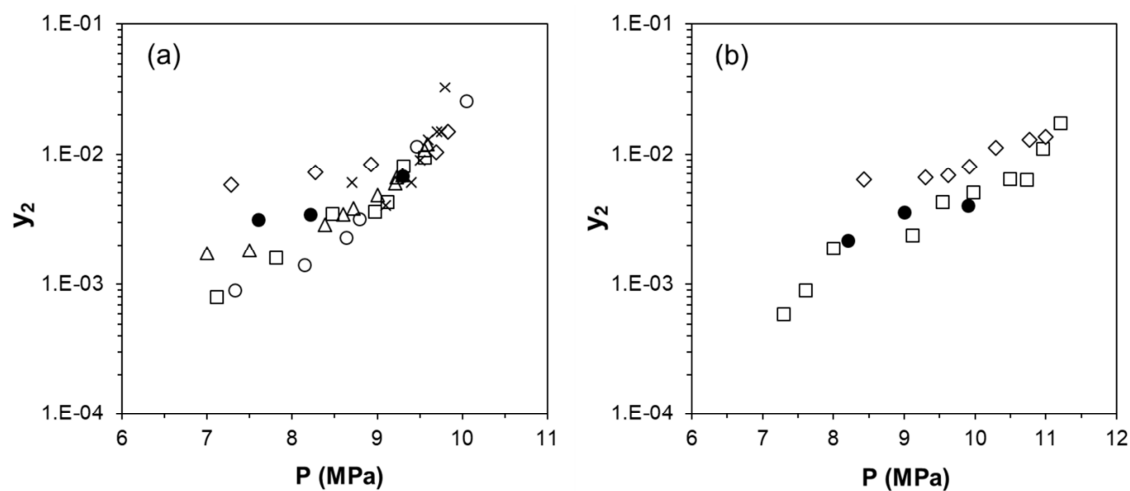


Figure 3. Solubility of liquid *D*-limonene in scCO_2 (y_2 , mole fraction) at (a) 50°C , and (b) 60°C . (●) This work, (□) Akgün et al. [46], (△) Sovová et al. [47], (◇) Chang and Chen [48], (○) Leeke et al. [49], (×) Matos et al. [50].

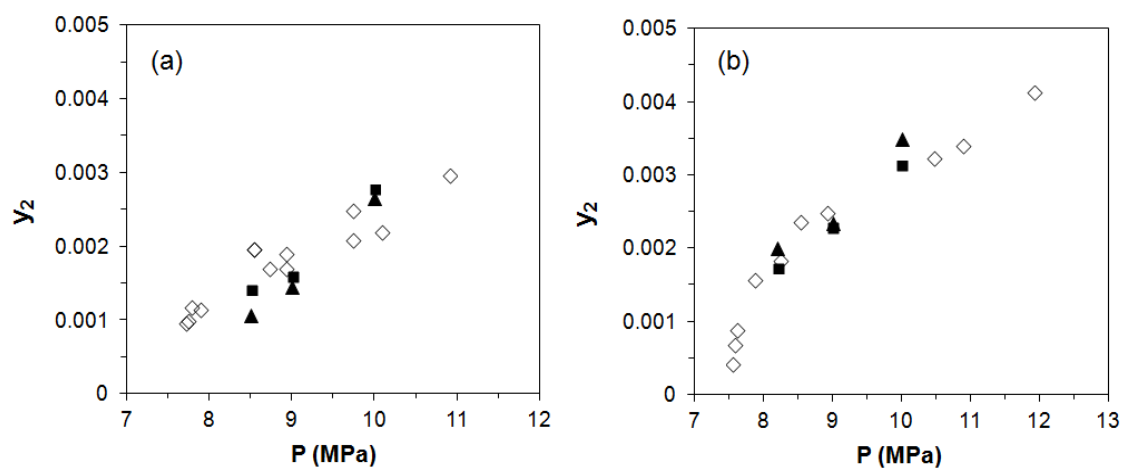


Figure 4. Solubility of solid diphenylamine in scCO₂ (y_2 , mole fraction) at (a) 32°C, and (b) 37°C. (▲) This work, spectrophotometric; (■) this work, gravimetric; (◇) Tsekhanskaya et al. [51], gravimetric.

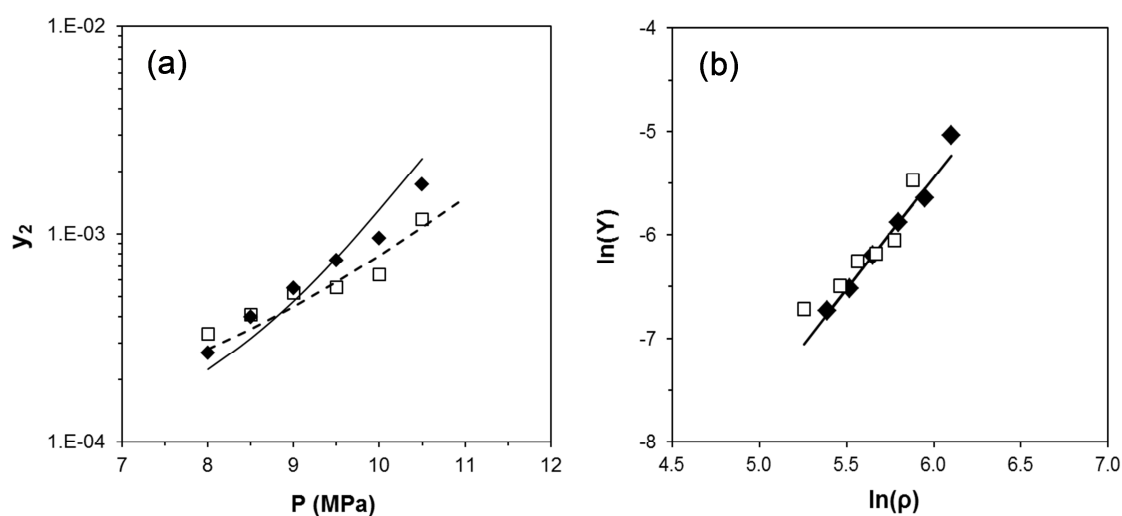


Figure 5. Solubility of liquid thymoquinone in scCO₂ (y_2 , mole fraction) as a function of pressure. Experimental values at: (◆) 50°C, (□) 60°C. Lines: (a) GC-EoS predictions at: (—) 50°C, (---) 60°C; (b) Chrastil model fit. Y : thymoquinone mass fraction in scCO₂; ρ : pure CO₂ density (kg/m³).

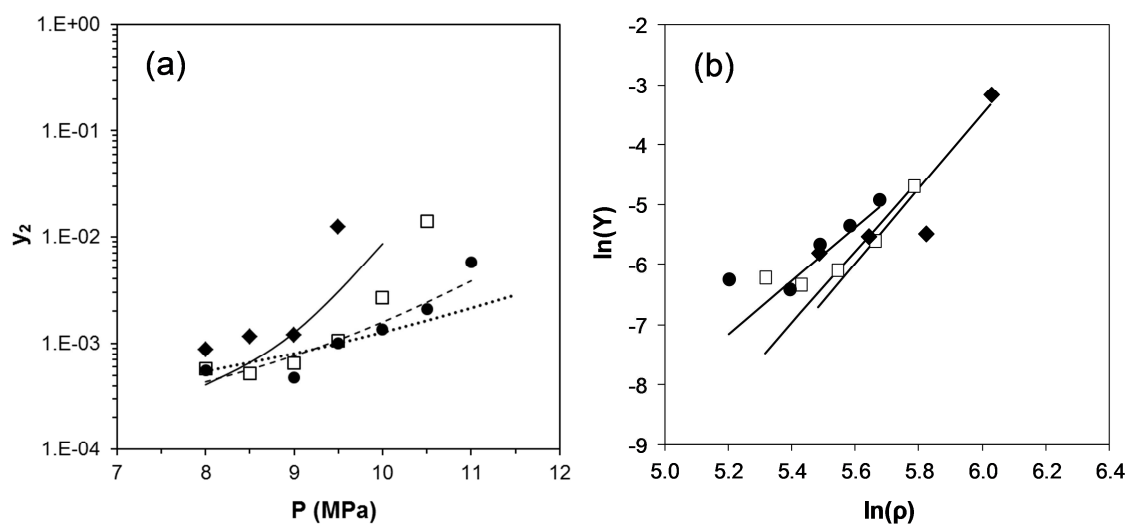


Figure 6. Solubility of liquid *R*-(+)-pulegone in scCO₂ (y_2 , mole fraction) as a function of pressure. Experimental values at: (◆) 45°C, (□) 55°C, (●) 65°C. Lines: (a) GC-EoS predictions at: (—) 45°C, (---) 55°C, (···) 65°C; (b) Chrastil model fit. Y : *R*-(+)-pulegone mass fraction in scCO₂; ρ : pure CO₂ density (kg/m³).

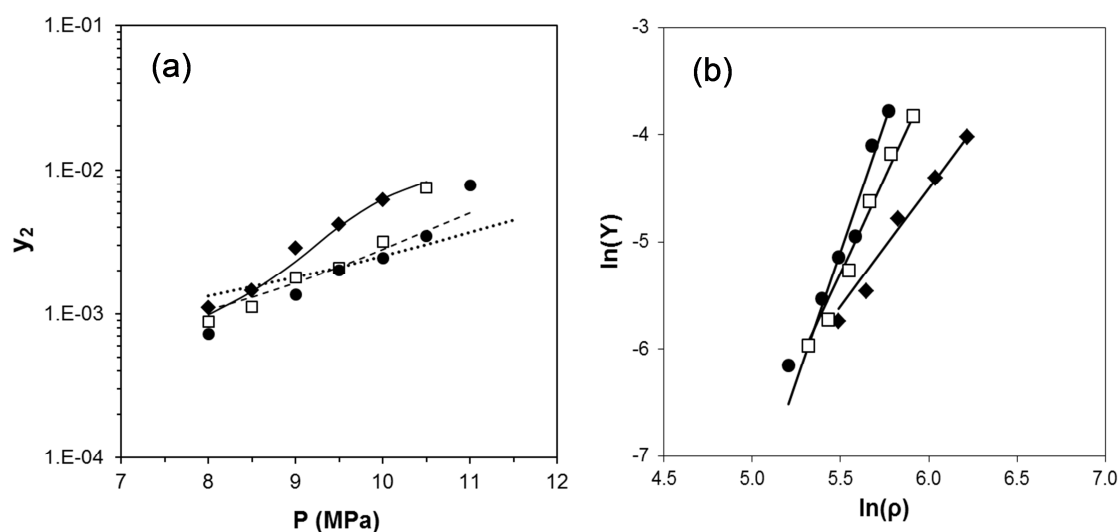


Figure 7. Solubility of liquid 1-octen-3-ol in $scCO_2$ (y_2 , mole fraction) as a function of pressure. Experimental values at: (◆) 45°C, (□) 55°C, (●) 65°C. Lines: (a) GC-EoS predictions at: (—) 45°C, (---) 55°C, (···) 65°C; (b) Chrastil model fit. Y : 1-octen-3-ol mass fraction in $scCO_2$; ρ : pure CO_2 density (kg/m^3).